

Supplementary Information

High efficiency of solution-processed inverted organic solar cells enabled by an aluminum oxide conjunction structure

Yi Yang, Mengqi Cui, Zhengyan Jiang, Ruijia Zhang, Xinjun He, Hui Liu, Biao Zhou and Wallace C.H. Choy*

Department of Electrical and Electronic Engineering, The University of Hong Kong, Pokfulam Road, Hong Kong, China.

*corresponding author email: chchoy@eee.hku.hk

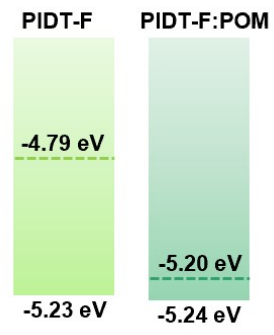


Fig. S1. The energy diagram of PIDT-F and PIDT-F:POM.

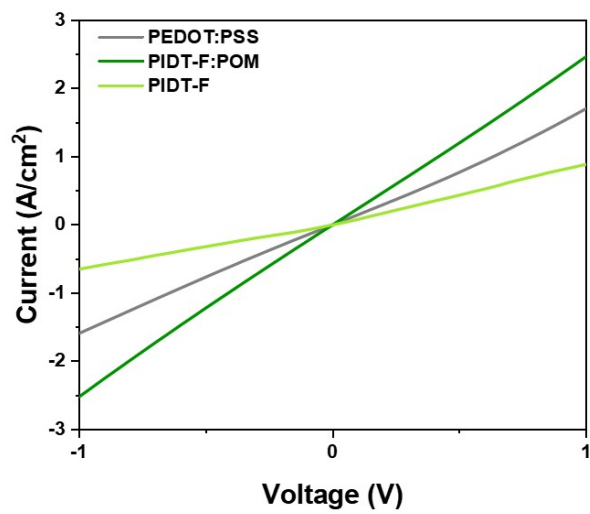


Fig. S2. The *J-V* characteristic of ITO/HTL/Ag.

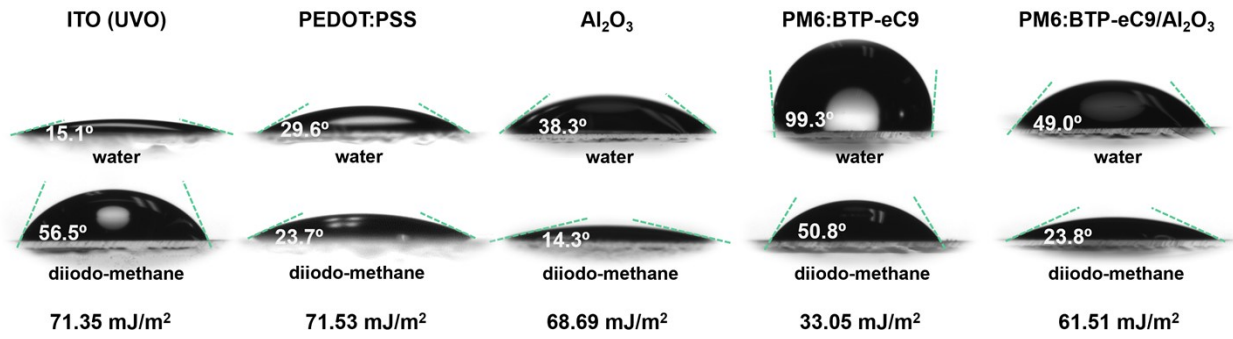


Fig. S3. The contact angle of water and diiodo-methane on different substrates.

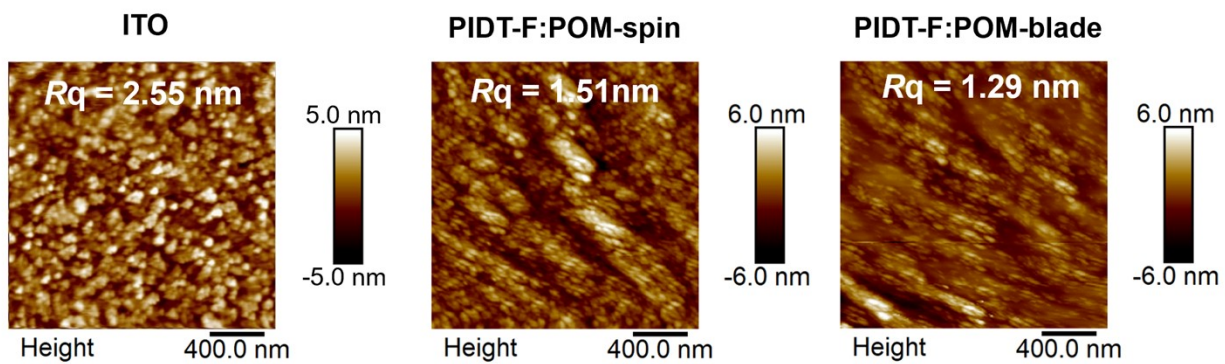


Fig. S4. AFM height image of ITO and ITO/spin-coated PIDT-F:POM and ITO/blade-coated PIDT-F:POM.

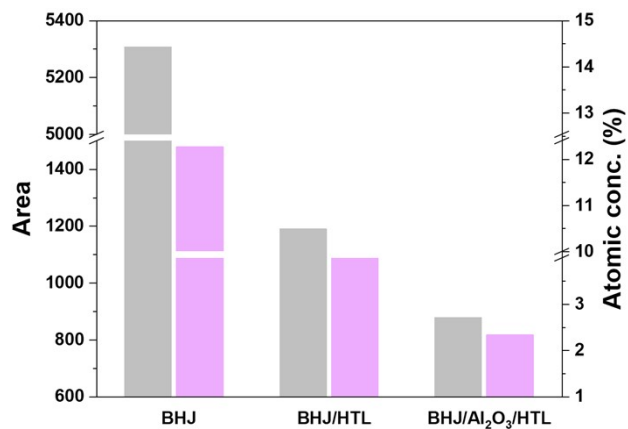


Fig. S5. The integral area and atomic concentration of Cl 2p of BHJ, BHJ/PIDT-F:POM and BHJ/Al₂O₃/PIDT-F:POM films. The atomic concentration refers to the content of Cl to total content of N, S, Cl, Al.

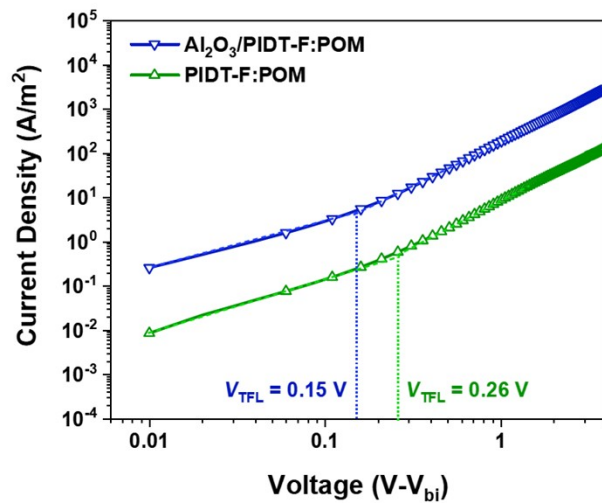


Fig. S6. Space charge limited current of hole-only devices based on PIDT-F:POM and Al₂O₃/PIDT-F:POM.

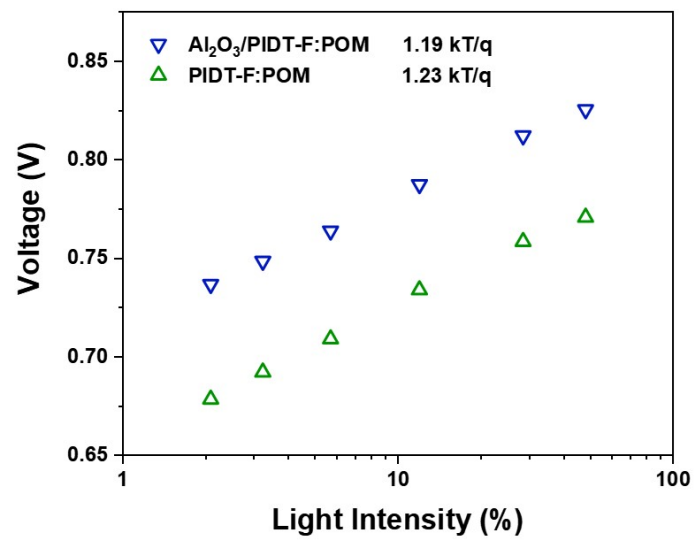


Fig. S7. Light intensity dependence of V_{OC} of PIDT-F:POM and Al₂O₃/PIDT-F:POM based devices.

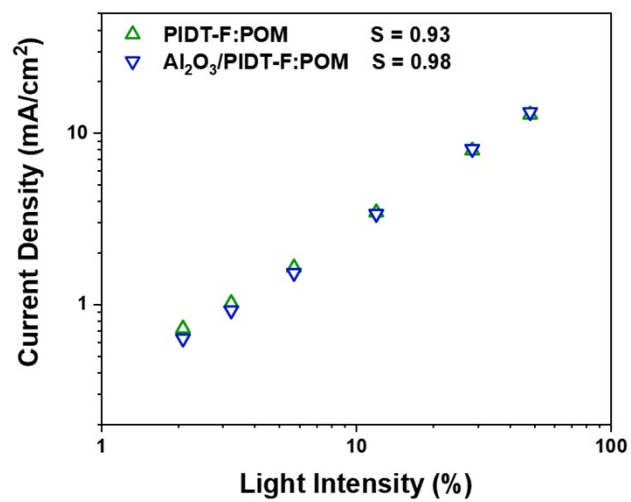


Fig. S8. Light intensity dependence of J_{SC} of PIDT-F:POM and $\text{Al}_2\text{O}_3/\text{PIDT-F:POM}$ based devices.

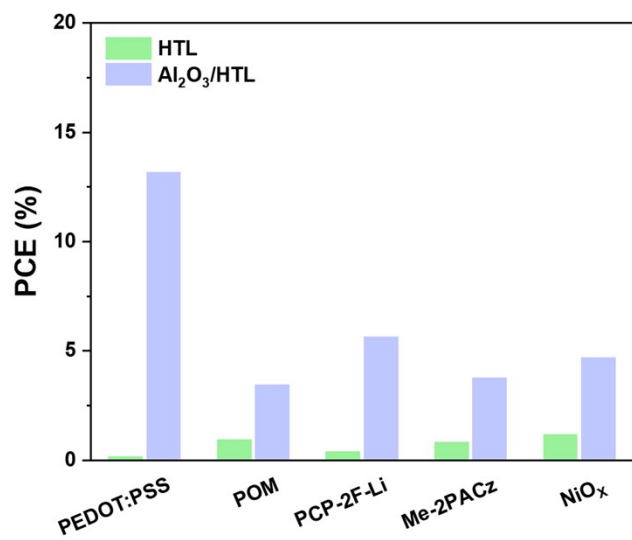


Fig. S9. PCE of inverted OSCs based on different HTLs with or without the Al₂O₃ buffer layer.

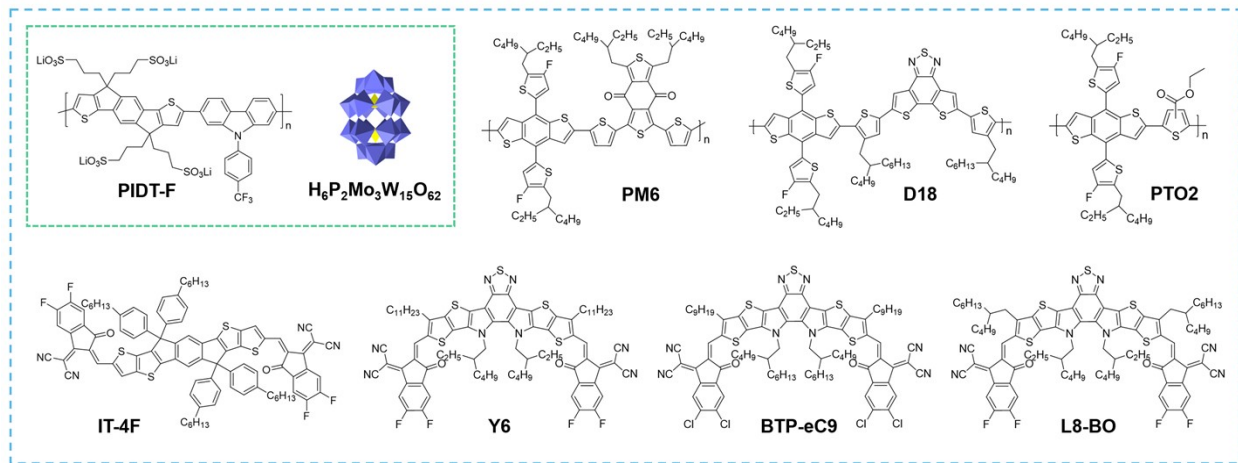


Fig. S10. The chemical structures of PIDT-F, POM, and active layer materials.

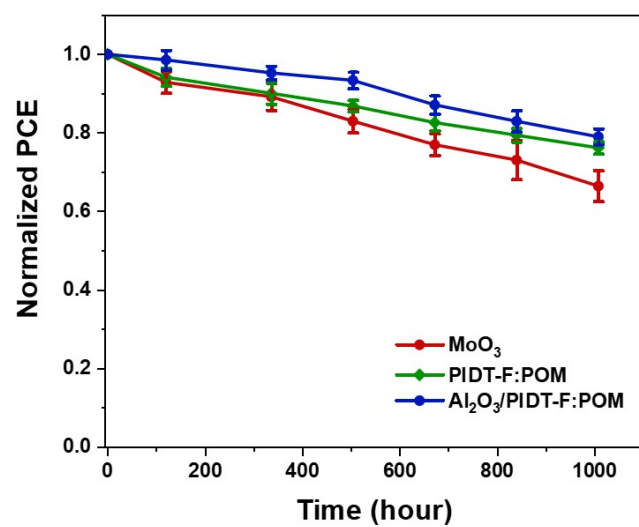


Fig. S11. The storage stability with variance of MoO₃ and Al₂O₃/PIDT-F:POM based devices with encapsulation (Fig. 4c).

Table 1. Photovoltaic parameters of conventional OSCs based on PM6:BTP-eC9 using different HTLs.

HTL	V_{oc} (V)	J_{sc} (mA/cm ²)	FF	PCE (%) ^{a)}
PEDOT:PSS	0.847	26.9	0.766	17.5 (17.3±0.2%)
PIDT-F:POM	0.855	26.8	0.771	17.6 (17.5±0.2%)

^{a)} The average values are calculated based on 12 individual devices shown in the brackets.

Table S2. Photovoltaic parameters of inverted OSCs based on PM6:BTP-eC9 using different HTLs.

HTL	V_{oc} (V)	J_{sc} (mA/cm ²)	FF	PCE (%) ^{a)}
MoO ₃	0.838	26.9	0.743	16.7 (16.2±0.3%)
PIDT-F:POM	0.815	26.6	0.733	15.9 (15.8±0.1%)
Al ₂ O ₃ /PIDT-F:POM	0.849	27.0	0.752	17.2 (17.1±0.1%)

a) The average values are calculated based on 12 individual devices shown in the brackets.

Table S3. The photovoltaic parameters of inverted devices with different HTLs.

HTL	V_{oc} (V)	J_{sc} (mA/cm ²)	FF	PCE (%)
PEDOT:PSS	0.05	12.5	0.26	0.15
Al ₂ O ₃ /PEDOT:PSS	0.79	25.4	0.68	13.2
PCP-2F-Li	0.19	6.57	0.31	0.39
Al ₂ O ₃ /PCP-2F-Li	0.47	23.4	0.51	5.65
Me-2PACz	0.13	19.3	0.33	0.82
Al ₂ O ₃ /Me-2PACz	0.39	22.6	0.43	3.78
NiO _x	0.16	19.8	0.36	1.17
Al ₂ O ₃ /NiO _x	0.43	23.22	0.47	4.70

Table S4. The photovoltaic parameters of inverted devices with different active layers.

Active layer	HTL	V_{oc} (V)	J_{sc} (mA/cm ²)	FF	PCE (%)
PM6:IT-4F	MoO ₃	0.85	19.1	0.75	12.2
	Al ₂ O ₃ /PIDT-F:POM	0.85	19.5	0.75	12.5
PTO2:IT-4F	MoO ₃	0.90	20.3	0.70	12.8
	Al ₂ O ₃ /PIDT-F:POM	0.91	20.7	0.71	13.4
PM6:Y6	MoO ₃	0.83	25.8	0.74	15.9
	Al ₂ O ₃ /PIDT-F:POM	0.84	25.7	0.75	16.2
PM6:D18:L8-BO	MoO ₃	0.88	26.4	0.75	17.5
	Al ₂ O ₃ /PIDT-F:POM	0.89	27.0	0.76	18.4

Table S5. Some representative inverted OSCs with solution-processed HTLs.

BHJ	HTL	V_{oc} (V)	J_{sc} (mA/cm ²)	FF	PCE (%)	DOI
P3HT:PCBM	NiO	0.58	10.07	51	3.01	10.5012/bkcs.2011.32.3.1067
a-PTPTBT:PCBM	VO _x	0.82	11.6	53	5.0	10.1002/adma.201102142
P3HT:PCBM	PEDOT:CFS-31	0.607	7.8	65.4	3.1	10.1039/c2jm35646e
PTB7-F20:PC ₇₁ BM	PEDOT:PSS + Au NPs	0.640	17.068	64.0	7.430	10.1039/c2ee23359b
P3HT:PCBM	AgNPs	0.386	7.39	38.5	1.1	10.7567/JJAP.52.04CR13
P3HT:PCBM	PFT-3HT	0.60	11.3	64.9	4.6	10.1021/cm400297p
PSEHTT:ICBA	Polyaniline (PANI)	0.89	11.60	66.87	6.87	10.1039/c3nr03011c
P3HT:PCBM	V ₂ O ₅	0.563±0.015	10.69±0.38	50.49±1.90	3.09±0.18	10.1039/c3ee42204f
PTB7:PC ₇₁ BM	MoS ₂	0.72	15.90	71	8.11	10.1002/aenm201300549
PTTh ₄ FBT:PC ₇₁ BM	sGO/VO _x	0.76	13.2	67	6.7	10.1002/aenm.201300430
P3HT:ICBA	PEDOT:PSS CPP	0.79±0.01	9.2±0.4	56±2	4.0±0.3	10.1002/adfm.201303232
PTB7:PC ₇₁ BM	tungsten carbide (WC)	0.72	15.98	70	8.04	10.1039/c3ta13473c
PIDTT-DFBT-TT:PC ₇₁ BM	graphene oxide (GO)	0.958	11.6	49.3	5.50	10.1002/adfm.201302426
P3HT:PCBM	PEDOT:PSS	0.540	9.13	62.9	3.10	10.1016/j.solmat.2014.07.007
P3HT:IC ₇₀ BA	PEDOT:PSS:V ₂ O ₅	0.87	7.53	64.1	4.20	10.1016/j.solmat.2013.09.009
P3HT:PCBM	PEDOT:PSS-AuNP	0.47	6.2	48	1.4	10.1002/pssa.201330674
P3HT:PCBM	TiOPc	0.48	3.5	50	0.84	10.1002/pssa.201431068
P3HT:PC ₆₀ BM	Nafion-modified MoO _x	0.60	9.65	60.34	3.49	10.1021/am507459t
P3HT:PCBM	V ₂ O ₅	0.570	3.20	30	0.55	10.1016/j.optmat.2015.10.036
P3HT:PCBM	CoO _x	0.57	8.95	53	2.72	10.1088/0268-1242/30/5/055001
P3HT:PC ₆₁ BM	V ₂ O ₅	0.60	9.22	58.02	3.21	10.1038/lisa.2015.46
PTB7:PC ₆₁ BM	MoO ₃ :PEDOT:PSS	0.74	12.7	63	5.92	10.1021/am509049t

P3HT:PC ₆₁ BM	V ₂ O _x	0.58±0.02	8.22±0.51	61±3	2.89±0.21	10.1063/1.4966806
PCE-10:PC ₆₀ BM	PEDOT:PSS:MoO _x	0.78	14.99	63	7.39	10.1002/aenm.201601959
P3HT:PC ₇₀ BM	PEDOT:PSS:ZD	0.582±0.007	9.26±0.38	58.26±2.56	3.16±0.15	10.1021/acsami.7b01183
PffBT4T-2OD:PC ₇₁ BM	PMA:PEDOT:PSS	0.77	18.4	64	9.07	10.1021/acsami.7b13346
PTB7-Th:PC ₇₁ BM	L-GO:NiO _x	0.78±0.00	19.16±0.33	65±1	9.73±0.08 (9.93)	10.1002/adfm.201706403
PTB7-Th:PC ₇₁ BM	Graphene-MoS ₂	0.80	17.1	67.7	9.5	10.1016/j.carbon.2018.10.038
SMD2:ITIC-Th	WO ₃ /PEDOT:PSS	0.899	17.3	66.0	10.3	10.1002/aenm.201902065
PBDB-T-2F:IDIC:Y6	H _x MoO ₃ /PEDOT:PSS	0.83	21.0	0.68	11.9	10.1002/adma.201907840
PTB7-Th:EH-IDTBR	S-FrGO	1.00	15.46	59.8	9.27	10.1021/acsami.0c11384
PBDB-T-2F:IT-4F	Cu-NiO _x (12.2%)+F4-TCNQ	0.827	18	53.3	7.92	10.1039/d0qm00619j
PTB7:PC ₇₁ BM	VO _x -PEDOT	0.80	20.06	54	8.6	10.1038/s41598-021-93365-8
PTB7-Th:IEICO-4F	NiO	0.719	23.99	65.1	11.23	10.1002/sml.202101729
PM6:PC ₇₁ BM:BTP-eC9	PEDOT:F	0.85	26.01	77	17.02	10.1038/s41560-022-00997-9
PBDB-T-2F:Y6	Cl ₂ -CuSCN	0.84	25.5	72.0	15.4	10.1021/acsenergylett.2c01545
P3HT:PCBM	m-PEDOT:PSS/GO	0.62	13.00	51.14	4.13	10.1016/j.orgel.2021.106388
PV2000:PC ₇₁ BM	PMA:PEDOT:PSS	0.804	15.6	72.2	9.01	10.1002/aesr.202300006
PM6:Y6	NiO _x :PMMA	0.853±0.006	24.92±0.13	70.33±0.45	14.95±0.12 (15.11)	10.3390/polym15081875
P3HT:PCBM	graphene	0.51±0.01	7.44±0.11	48±3	1.82±0.14 (2.00)	10.3390/mi14101858
PM6:Y6	BCF-Li doped PCE12np	0.85	22.29	0.72	13.66	10.1021/acsenergylett.3c02087
PM6:BTP-eC9:L8-BO	D-PTAA np/PEDOT:PSS	0.85	28.03	71.4	17.06	10.1016/j.joule.2024.06.013

Table S6. The photovoltaic parameters of OSCs with different HTLs.

Device structure-HTL ^{a)}	V _{oc} (V)	J _{sc} (mA/cm ²)	FF	PCE (%)
<i>c</i> -PIDT-F	0.81	27.2	0.59	13.0
<i>i</i> -PIDT-F	0.37	25.9	0.36	3.51
<i>i</i> -Al ₂ O ₃ /PIDT-F	0.64	26.4	0.61	10.2
<i>c</i> -PIDT-F:POM (1:1)	0.84	26.3	0.77	17.0
<i>i</i> -PIDT-F:POM (1:1)	0.73	26.7	0.43	8.41
<i>i</i> -Al ₂ O ₃ /PIDT-F:POM (1:1)	0.83	26.1	0.72	15.6
<i>c</i> -PIDT-F:POM (1:2)	0.84	26.6	0.77	17.3
<i>i</i> -PIDT-F:POM (1:2)	0.81	26.9	0.73	15.8
<i>i</i> -Al ₂ O ₃ /PIDT-F:POM (1:2)	0.84	27.0	0.76	17.1
<i>c</i> -PIDT-F:POM (1:3)	0.86	26.8	0.77	17.6
<i>i</i> -PIDT-F:POM (1:3)	0.81	26.6	0.73	15.9
<i>i</i> -Al ₂ O ₃ /PIDT-F:POM (1:3)	0.85	27.0	0.75	17.2
<i>c</i> -PIDT-F:POM (1:5)	0.84	26.7	0.78	17.5
<i>i</i> -PIDT-F:POM (1:5)	0.80	26.5	0.72	15.2
<i>i</i> -Al ₂ O ₃ /PIDT-F:POM (1:5)	0.84	27.2	0.72	16.6
<i>c</i> -POM	0.85	26.4	0.78	17.4
<i>i</i> -POM	0.12	22.5	0.34	0.94
<i>i</i> -Al ₂ O ₃ /POM	0.31	25.6	0.43	3.46

^{a)} *c*- for conventional structure (ITO/HTL/PM6:BTP-eC9/PFN-Br/Ag); *i*- for inverted structure (ITO/ZnO/PM6:BTP-eC9/HTL/Ag).

Table S7. The photovoltaic parameters of 1cm² OSC based on PM6:BTP-eC9.

HTL	V _{oc} (V)	J _{sc} (mA/cm ²)	FF	PCE (%)
PIDT-F:POM	0.85	27.2	0.72	16.6

The compatibility of PIDT-F:POM with large-area blade-coating techniques is investigated. First, we prepare a PIDT-F:POM film via blade-coating and characterize its surface morphology by AFM. As shown in Supplementary Fig. 4, the blade-coated PIDT-F:POM film exhibits a smooth surface with a low R_q of 1.29 nm, which is quite similar to the spin-coated film. The 1 cm² OSC device with the blade-coated PIDT-F:POM shows a decent PCE of 16.6%. (Supplementary Table 5) The results imply that PIDT-F:POM is compatible with the large-area processing method, making it a promising candidate for practical application.